

# Flame-Retardant Mechanism of Silica: Effects of Resin Molecular Weight

Takashi Kashiwagi, John R. Shields, Richard H. Harris, Jr., Rick D. Davis

Building and Fire Research Laboratory, National Institute of Standards and Technology, Gaithersburg, Maryland 20899-8665

Received 8 January 2002; accepted 27 January 2002

**ABSTRACT:** The effects of resin molecular weight on the flame-retardant mechanism of silica were studied with two different molecular weights of poly(methyl methacrylate) (PMMA), 122,000 and 996,000 g/mol, and two silicas, fused silica with a small surface area and silica gel with a large surface area. A total of six different samples were studied, with a mass fraction of 10% silica. The mass loss rate of the six samples in nitrogen and the heat release rate from burning in air were measured at an external radiant flux of 40 kW/m<sup>2</sup>. The addition of silica gel to the low-molecular-weight PMMA significantly reduced the mass loss rate and heat release rate; addition to the high-molecular-weight PMMA provided the largest reductions of these quantities in this study. For fused silica, some reduction in mass loss rate

and heat release rate was observed when it was added to the high-molecular-weight PMMA; addition to the low-molecular-weight PMMA did not reduce either loss rate. Chemical analysis of the collected residues and observation of the sample surface during gasification reveal the accumulation of silica near the surface; the larger its coverage over the sample surface was, less the mass loss rate and heat release rate were. Both the level of accumulation and its surface coverage depended strongly not only on the silica characteristics but also on the melt viscosity of the PMMA. © 2002 Wiley Periodicals, Inc. *J Appl Polym Sci* 87: 1541–1553, 2003

**Key words:** silicas; flame retardance; resins; melt

## INTRODUCTION

As an alternative to the use of halogenated flame retardants, which reduce the flammability of polymeric materials by modification of the gas-phase oxidation chemistry in the flame,<sup>1</sup> our approach has been to modify the condensed-phase chemistry and/or physical processes of burning polymeric materials by the addition of inorganic additives.<sup>2–5</sup> In our previous study,<sup>5</sup> various types of silica, silica gel, fumed silicas, and fused silica were added to polypropylene (PP) and poly(ethylene oxide) to determine their flame-retardant effectiveness and mechanisms of flame retardancy in filled materials. The addition of low-density silicas with large surface areas (e.g., fumed silicas and silica gel) to these polymers significantly reduced the heat release and burning rates. However, the addition of fused silica did not reduce the flammability properties as much as the other silicas. It was postulated in the previous study that fumed silica particles

and silica gel particles accumulated near the surface to act as a thermal insulation layer and also acted to reduce the polymer concentration near the surface, creating a less flammable material. Moreover, it was suggested that the denser, fused silica particles drifted through the polymer melt layer and did not accumulate near the surface.<sup>5</sup>

This study further examined this hypothesis by the determination of the effects of polymer melt viscosity on the flammability properties of poly(methyl methacrylate) (PMMA) with the addition of the various silicas. The selection of PMMA was based on its large average *zip length* (the average number of monomer units produced from a chain scission initiation), above 1000.<sup>6</sup> Therefore, the molecular weight of PMMA does not significantly change during thermal degradation (burning). This means that high-molecular-weight poly(methyl methacrylate) (HMWPMMA) samples remain highly viscous and low-molecular-weight poly(methyl methacrylate) (LMWPMMA) samples remain much less viscous at high temperatures during thermal degradation. Therefore, the effects of melt viscosity can be determined by comparison of the flammability properties of LMWPMMA (low melt viscosity) with the addition of silica gel and fused silica to that of HMWPMMA (high melt viscosity) with the addition of the same two silicas. If the hypothesis is correct, the addition of silica gel to the HMWPMMA should significantly reduce the heat release rate of the PMMA,

According to ISO 31-8, the term *molecular weight* has been replaced with *relative molecular mass*, ( $M_r$ ) The conventional notation, rather than the ISO notation, is used in this article.

Correspondence to: T. Kashiwagi (takashi.kashiwagi@nist.gov).

whereas the addition of fused silica should yield a much smaller reduction of the heat release rate. Furthermore, for LMWPMMA, the addition of silica gel should less effectively reduce the heat release rate.

## EXPERIMENTAL

### Materials

Two powder PMMA samples (Aldrich,\* Milwaukee, WI) were used with reported mass-average molecular weights ( $M_w$ 's) of 120,000 and 996,000 g/mol. The silica gel (PQ Corp., Valley Forge, PA) had a pore volume of 2.0 cm<sup>3</sup>/g, an average particle size of 17  $\mu$ m, and a surface area of 400  $\pm$  40 m<sup>2</sup>/g. The samples were heated at 900°C for 2 h. The selection of this silica gel was made on the basis of the results of our previous study, which determined the effects of various silica gel characteristics, such as particle size, pore volume, surface area, and silanol content, on the flammability properties of PP.<sup>7</sup> The fused silica was Siltex 44C (Kaopolite, Inc., Union, NJ) with near-zero pore volume and an average particle size of 7  $\mu$ m. It was heated at 100°C for 2 h. All samples had a PMMA mass fraction of 90% and a silica mass fraction of 10%. The samples were mixed by vigorous steering in a mortar with a pestle for 3 min. The sample disks were made by compression molding at 190°C for the LMWPMMA samples, and at 210°C for the HMWPMMA samples. All HMWPMMA samples used in this study were 75 mm in diameter and 8 mm thick; all LMWPMMA samples were 75 mm in diameter and 5 mm thick.

### Analysis of samples

#### Thermal stability measurement

Sample mass as a function of temperature was obtained with a TA Instruments SDT 2960 at a heating rate of 5°C/min in a nitrogen atmosphere. The standard uncertainty on sample mass measurement was  $\pm$ 1%.

#### Viscosity measurement

Viscosities of the samples were measured with a Paar Physica UDS 200 viscometer at an oscillation frequency of 1 Hz from 180 to 240°C at a heating rate of 2°C/min in a nitrogen atmosphere. The standard uncertainty of the measured melt viscosity was  $\pm$ 15%.

\* Certain commercial equipment, instruments, materials, services or companies are identified in this article to specify adequately the experimental procedure. This in no way implies endorsement or recommendation by the National Institutes of Standards and Technology (NIST).

### Cone calorimeter test

The flammability properties, including heat release rate, mass loss rate, and others, were measured with a cone calorimeter (made by NIST) at 40 kW/m<sup>2</sup> in accord with ASTM E 1356. The standard uncertainty of the measured heat release rate<sup>2</sup> was  $\pm$ 10%. All test samples were horizontal.

### Gasification rate measurement

A radiant gasification apparatus, somewhat similar to the cone calorimeter, was designed and constructed at NIST to study the gasification processes of samples by the measurement of mass loss rate and temperatures of the sample in a nitrogen atmosphere (no burning). All experiments were conducted at 40 kW/m<sup>2</sup>. The unique nature of this device is threefold: (1) observation and results obtained from it are only based on the condensed-phase processes due to the absence of any gas-phase oxidation reactions and processes; (2) it enables visual observations of gasification behavior of a sample with a video camera under a radiant flux similar to that of a fire without any interference from a flame; and (3) the external flux to the sample surface is well-defined and nearly constant over the duration of entire experiment (and over the spatial extent of the sample surface) due to the absence of heat feedback from a flame. A more detailed discussion of the apparatus was given in our previous study; the standard uncertainty of the measured mass loss rate<sup>8</sup> was within 10%.

### Silicon, carbon, and hydrogen analyses

Si contents in the collected sample residues were measured by neutron activation analysis, and C and H contents in the residues were measured by elemental analysis with a LECO instrument. All these measurements were conducted at the Dow Chemical Co.

## RESULTS

### Thermal analysis

Normalized sample mass loss rate divided by the heating rate is plotted in Figure 1 for the LMWPMMA samples and in Figure 2 for the HMWPMMA samples. It is known that radically polymerized PMMA starts to degrade by initiation at the head-to-head linkages, by initiation at the unsaturated ends, and by random initiation along the polymer backbone.<sup>9</sup> Generally, the contribution to sample mass loss from initiation at the head-to-head linkages is quite small. However, initiation from the unsaturated ends (at around 270°C) becomes more significant with a decrease in molecular weight due to an increase in the number of unsaturated ends initially present. The two large peaks shown

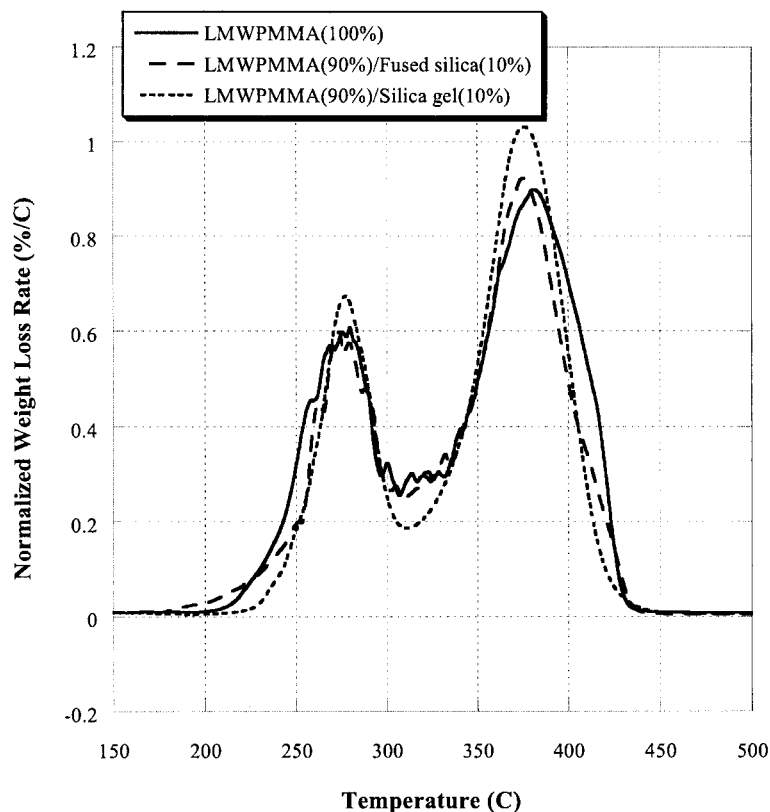


Figure 1 Derivative TGA of LMWPMMA with silicas at 5°C/m in nitrogen.

with the LMWPMMA corresponded to the latter two types of initiation, and the addition of the two types of silica did not appreciably modify the initiation steps or

the overall thermal stability of the LMWPMMA sample. For the HMWPMMA shown in Figure 2, the mass loss peak initiated from the unsaturated ends became

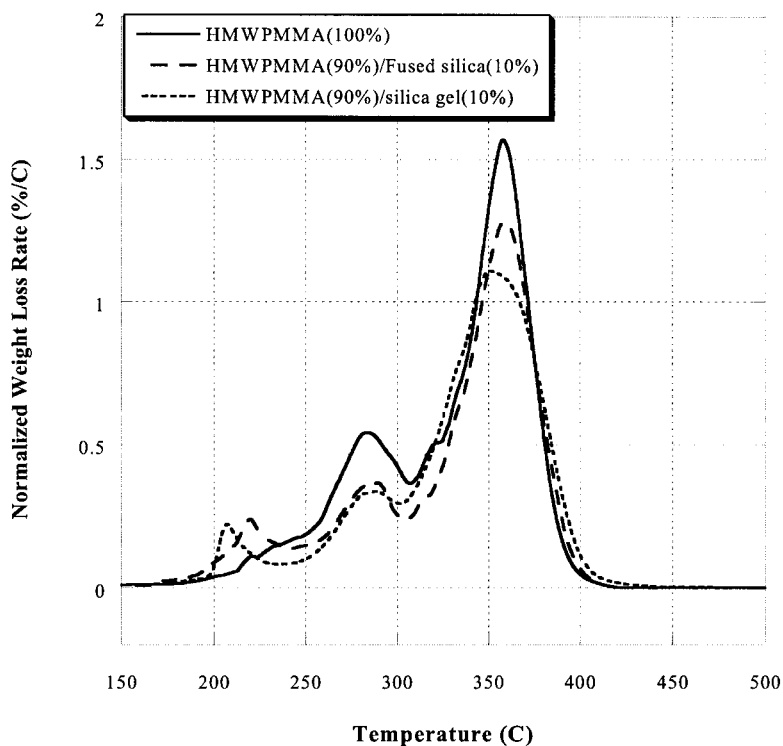


Figure 2 Derivative TGA of HMWPMMA with silicas at 5°C/m in nitrogen.

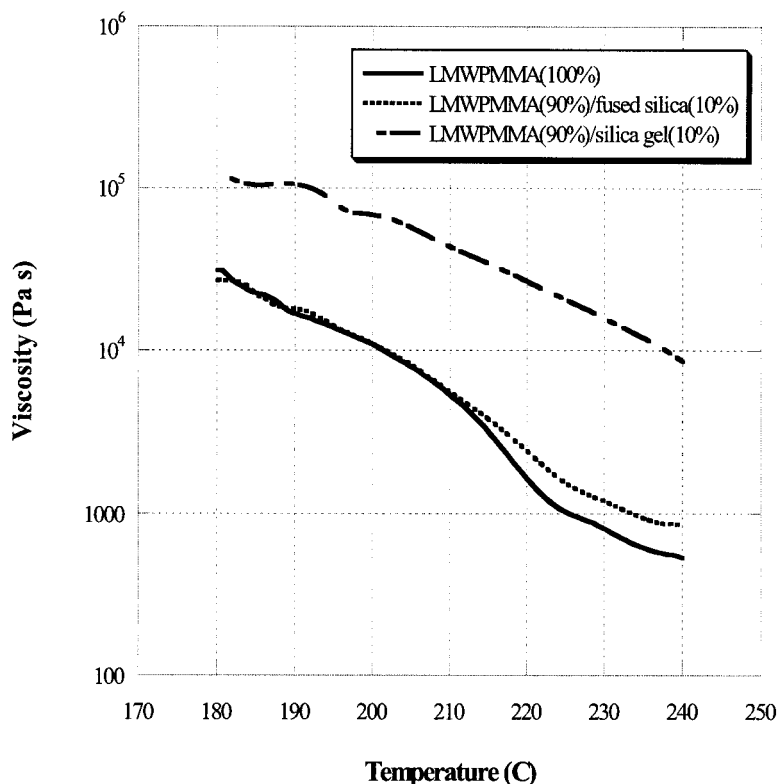


Figure 3 Melt viscosity versus temperature for LMWPMMA with silicas.

much smaller than that for LMWPMMA. The addition of the two types of silica to HMWPMMA yielded a new peak at around 210–220°C, which was compared with what was only a broad shoulder starting at about 210°C on the 270°C peak for unmodified HMWPMMA. Although it was not clear what reaction mechanism caused this new low-temperature peak seen with the addition of the silicas, the effects of the addition of the silicas on the overall thermal stability of HMWPMMA were not significant to the overall degradation behavior. Therefore, the observed differences described later for gasification rate and heat release rate among the PMMA samples and PMMA/silica samples did not appear to be mainly caused by a change in thermal stability brought on by the addition of the silicas to the PMMA samples.

All LMWPMMA samples were compression molded at 190°C, and no significant degradation of the samples was expected. However, all HMWPMMA samples were compression molded at 210°C, and a small amount of degradation occurred (in particular for samples with silica) corresponding to the small, first peak in Figure 2.

### Viscosity

The relationship between melt viscosity and temperature is shown in Figure 3 for the LMWPMMA samples and in Figure 4 for the HMWPMMA samples. The

melt viscosities of the LMWPMMA samples decreased sharply with an increase in temperature. The addition of the fused silica did not significantly increase the melt viscosity of LMWPMMA; however, the addition of the silica gel increased the melt viscosity roughly one order of magnitude over that of the pure LMWPMMA. At high temperatures, the melt viscosity of HMWPMMA was at least an order of magnitude higher than that of LMWPMMA, having decreased much more slowly with an increase in temperature than did the viscosity of LMWPMMA. The addition of the fused silica (10% mass fraction) did not significantly modify the melt viscosity of HMWPMMA, but the addition of the silica gel (10% mass fraction) increased the melt viscosity of HMWPMMA by roughly a factor of five. At elevated temperatures, the melt viscosities of all HMWPMMA samples were at least one order of magnitude higher than those of all LMWPMMA samples.

### Gasification

Observation of the sequence of events in the gasification of the pure LMWPMMA sample first revealed small bubbles at the sample surface around 30 s after irradiation, followed by the appearance of many large bubbles. Around 60 s, vigorous bubbling with many large bubbles was noted. The sample continued its vigorous bubbling, and the center portion of the sam-

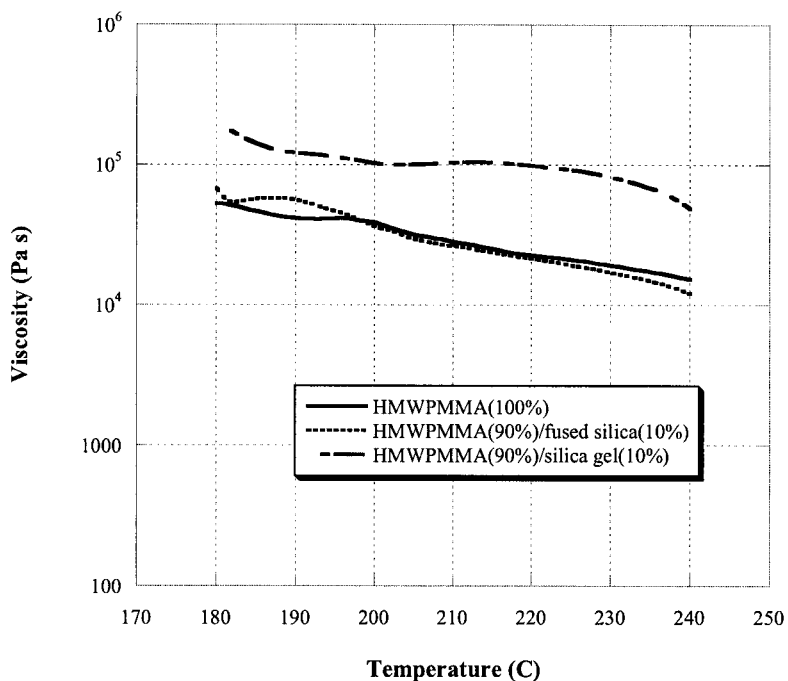


Figure 4 Melt viscosity versus temperature for HMWPMMA with silicas.

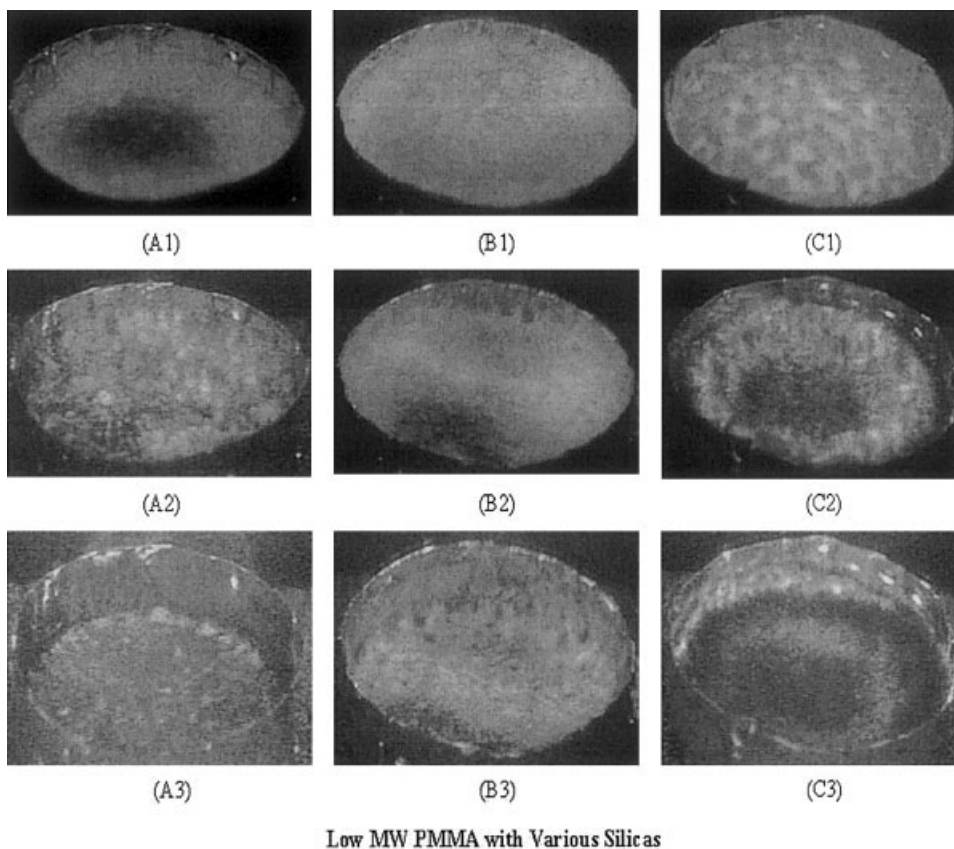


Figure 5 Selected sequence of images of the gasification phenomena of LMWPMMA samples with silicas in N<sub>2</sub> at 40 kW/m<sup>2</sup>: pure LMWPMMA at (A1) 120 s, (A2) 240 s, and (A3) 300 s; LMWPMMA (90%)/fused silica (10%) at (B1) 120 s (B2) 240 s, and (B3) 300 s. LMWPMMA (90%)/silica gel (10%) at (C1) 120 s (C2) 240 s, and (C3) 360 s.

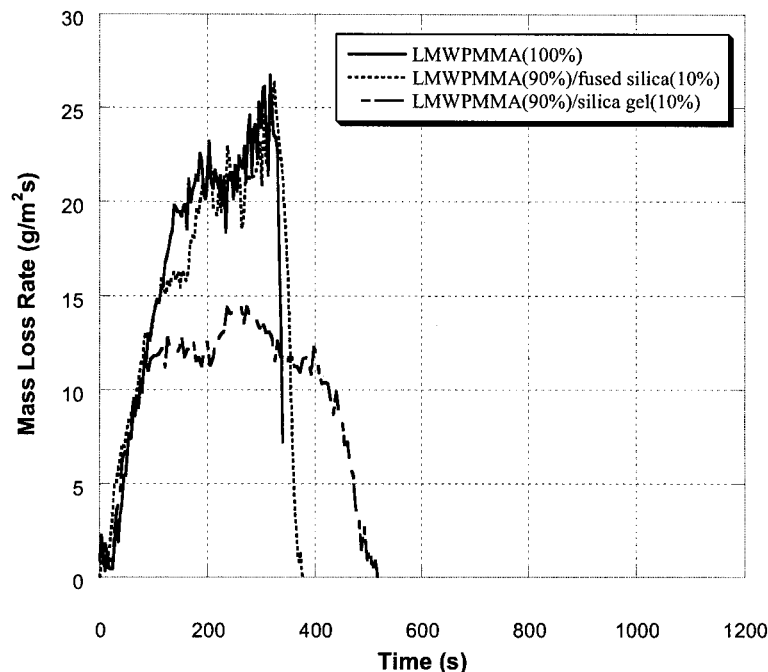


Figure 6 Effects of silica types on the mass loss rate of LMWPMMA in  $N_2$  at  $40 \text{ kW/m}^2$ .

ple surface became slightly dark in color at about 120 s, as shown in Figure 5(A1). After 120 s, more vigorous bubbling appeared, and the sample appeared less viscous (with the appearance of a fluid). Around 240 s, the surface was covered by bursting large bubbles (resembling a water surface hit by very heavy rain), as shown in Figure 5(A2). Vigorous bubbling with a very fluid sample continued, and the sample surface darkened after about 300 s. A very thin, black coating over the bottom of the container was left at the end of the test. The addition of the fused silica to LMWPMMA did not significantly change the gasification behavior of the pure LMWPMMA sample except that the sample appeared to be slightly more viscous. Sample swelling accompanied by release of bubbles, initiated after about 100 s, and these processes continued up to about 160 s. After 180 s, the gasification behavior was very similar to that of the pure LMWPMMA sample, and the remaining sample had very fluid behavior. A thin, dark gray crust-like layer was left at the bottom of the container at the end of the test. The mass of the residue was about the same as the initial mass of the added fused silica.

The gasification behavior of the LMWPMMA/silica gel sample was quite different from that of the previous samples. Many small, bubbles were observed around 30 s, but the sample appeared much more viscous. Many small, solid-looking islands appeared on the surface around 85 s, and bubbling was observed in the valleys between these islands. The solid islands grew laterally and connected to each other to cover the entire sample surface, as shown in Figure 5(C1). Swelling of this "solid" surface was observed

around 140 s, and the sample continued to slowly rise until it collapsed at around 210 s. The collapsed sample surface is shown in Figure 5(C2). The color of the surface became darker, and the fall of dark powders into the caved-in center of the sample was occasionally observed. A dark, relatively thick powdery layer [similar to the picture of Fig. 5(C3)] was left at the end of the test. The very fluid behavior observed for the previous two samples did not appear for this sample. The mass of the residue was almost the same as that of the initial weight of added silica gel, and the thickness of the residue was slightly less than that of the initial sample.

The calculated mass loss rates from the measured sample masses of all LMWPMMA samples are plotted in Figure 6. The mass loss rate curve of the LMWPMMA/fused silica sample was similar to that of the pure LMWPMMA sample, except between 100 and 200 s. This trend might have been expected from the similar observed thermal gravimetric results and physical gasification behavior of the two samples, described previously. The mass loss rate of the LMWPMMA/silica gel was roughly half of the value of the two samples, except at the early time up to about 60 s. However, the total sample mass loss (integrated values of the mass loss curves) was about the same for the three samples.

Observation of the gasification of the pure HMWPMMA sample first revealed the formation of numerous tiny bubbles at the sample surface around 30 s. Around 60 s, the sample surface appeared to be melting, and several larger bubbles were formed. However, the sample surface appeared solid-like with sev-

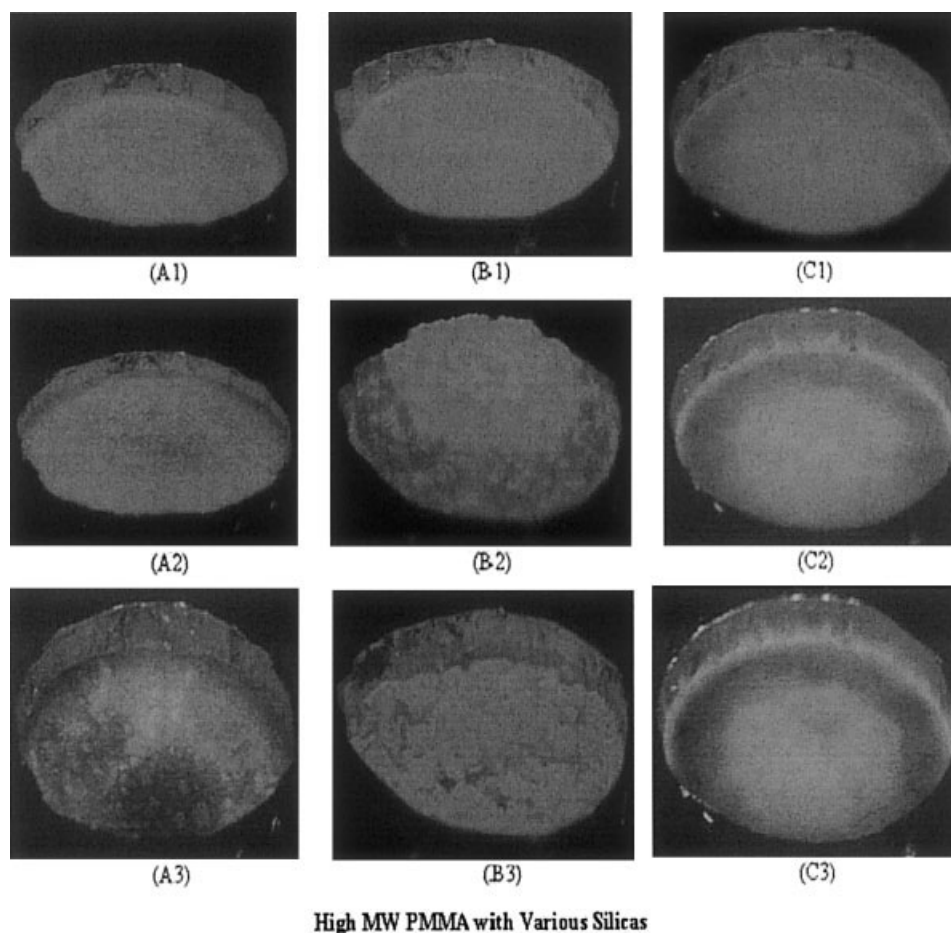


**Figure 7** Selected sequence of images of the gasification phenomena of HMWPMMA samples with silicas in  $N_2$  at  $40 \text{ kW/m}^2$ : Pure HMWPMMA at (A1) 120 s, (A2) 240 s, and (A3) 480 s; HMWPMMA (90%)/fused silica (10%) at (B1) 180 s (B2) 300 s, and (B3) 480 s; and HMWPMMA (90%)/silica gel (10%) at (C1) 180 s, (C2) 300 s, and (C3) 480 s.

eral bubbles, as shown in Figure 7(A1). The number of large bubbles gradually increased, and the sample appeared more fluid around 150 s. However, the size of the bubbles was smaller than those observed with the pure LMWPMMA sample. Swelling was observed around 260 s; then the surface continued to slowly rise up to 350 s. Then, the collapse of the swollen mound was observed around 360 s. After the collapse, the sample appeared to be more fluid, containing large bubbles. Little residue was left, except for several dark black spots at the bottom of the container, at the end of the test. The addition of the fused silica to HMWPMMA resulted in neither large bubble formation nor a fluid surface. Rather a white, snow-like surface with bright white islands was formed; bubbling occurred in the valleys between the white islands. Swelling was observed, and an elevated mound was formed, as shown in Figure 7(B2). During the collapse of the mound, numerous white, thin flakes were formed, as shown in Figure 7(B3). The residue consisted of white flakes ranging from several millimeters to 1 cm. The flakes were piled at the bottom of the sample container at the end of the test. The mass of the residue was

about 10% higher than that of the mass of fused silica in the initial sample. The HMWPMMA/silica gel sample did not reveal any bubbling or melting behavior during the entire test. The surface always appeared to be solid-like, and its color gradually became darker over the progress of the test, as shown in Figure 7(C1–C3). No sample surface recession and no significant visual changes in the sample were observed. The surface of the residue appeared to be pasty instead of powdery for the LMWPMMA/silica gel sample. The mass of the residue was about 20% higher than that of the silica gel in the initial sample.

The mass loss rate curves of all HMWPMMA samples are shown in Figure 8. The results show that even the addition of the fused silica significantly reduced the mass loss rate of HMWPMMA. The addition of silica gel was, however, more effective for mass loss rate reduction, reducing the peak rate to one third that of the pure sample. However, the total mass loss (integrated value of the mass loss curve) was about the same for all HMWPMMA samples. By comparing the mass loss rate curves shown in Figure 6 for the LMWPMMA samples, one sees that the addition of both

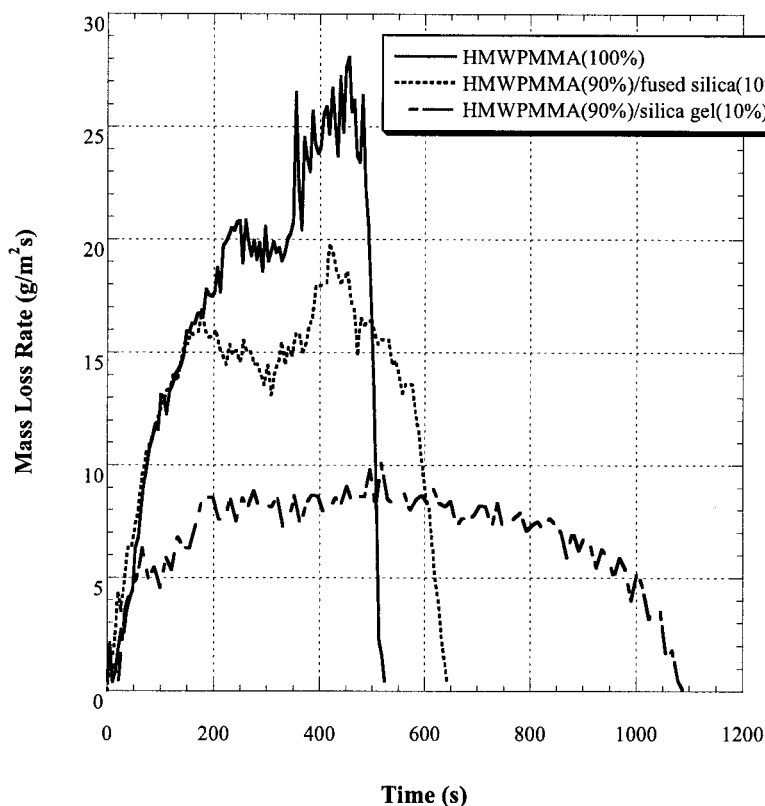


Figure 8 Effects of silica type on the mass loss rate of HMWPMMA in  $N_2$  at  $40 \text{ kW/m}^2$ .

types of silicas to the HMWPMMA sample yielded a greater mass loss rate reduction than this addition to the LMWPMMA sample.

#### Heat release rate

The heat release rates of all LMWPMMA samples are shown in Figure 9. The addition of the silica gel reduced the heat release rate of the LMWPMMA sample to roughly 50% of that of the pure sample, but the addition of the fused silica produced no significant reduction in heat release rate. The trends of the measured mass loss rate (burning rate) curves (not shown) were very close to those of the heat release curves, and thus, the calculated specific heat of combustion (measured heat release rate divided by measured mass loss rate) was  $24 \pm 2 \text{ MJ/kg}$  for the all LMWPMMA samples. Furthermore, the trends of the heat release rate curves were very similar to those of the mass loss rate in nitrogen, as shown in Figure 6.

The heat release rate curves of all HMWPMMA samples are shown in Figure 10. The trends shown in this figure are similar to those for the mass loss rate in nitrogen shown in Figure 8. The addition of the fused silica reduced the heat release rate about 25% compared to that for the pure HMWPMMA sample. The addition of the silica gel reduced the heat release rate of the HMWPMMA to about one third of the peak rate

of the pure sample. The calculated specific heat of combustion of all HMWPMMA samples was the same as that of the all LMWPMMA samples. The total heat release rate (heat release rate curve integrated over the test time) of both PMMA samples was about the same with or without the addition of silica.

#### DISCUSSION

When the surface of a thick PMMA sample is heated by an external source or by heat feedback from a flame, the temperature near the surface rapidly increases followed by reduction in viscosity of the sample near the surface. When the temperature of the sample becomes sufficiently high, degradation starts to generate methyl methacrylate (MMA) as the main degradation product.<sup>10</sup> Because the degradation temperatures of PMMA (shown in Figs. 1 and 2) are much higher than the boiling temperature of MMA ( $100^\circ\text{C}$ ), MMA is superheated and nucleates, forming bubbles in the melt layer. The bubbles rapidly rise (and expand) to the sample surface if the surrounding polymer layer is a melt with low viscosity. Thus, the mass loss rate and heat release rate (burning rate) of PMMA increase with the progress of the gasification and burning (the sample gets more heated in depth, and more sample gets degraded) as shown in Figures 6 and 8–10.

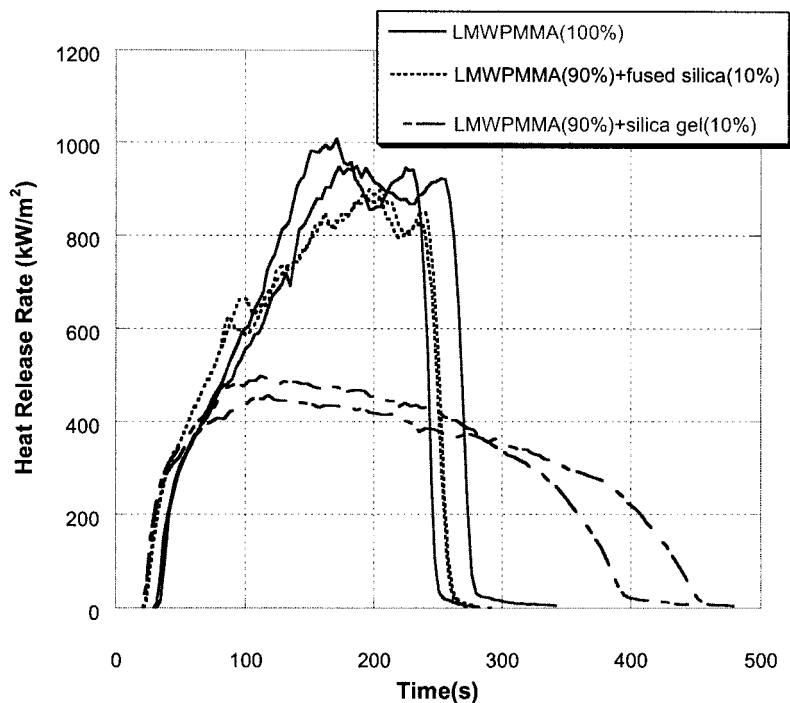


Figure 9 Effects of silica type on the heat release rate of LMWPMMA at 40 kW/m<sup>2</sup>.

The fused silica particles used in this study had nearly zero pore volumes and low surface areas. They had the appearance of light, fine sand. When the fused

silica was added to the LMWPMMA, the melt viscosity of the sample was still low enough so that the gasification of the LMWPMMA/fused silica sample

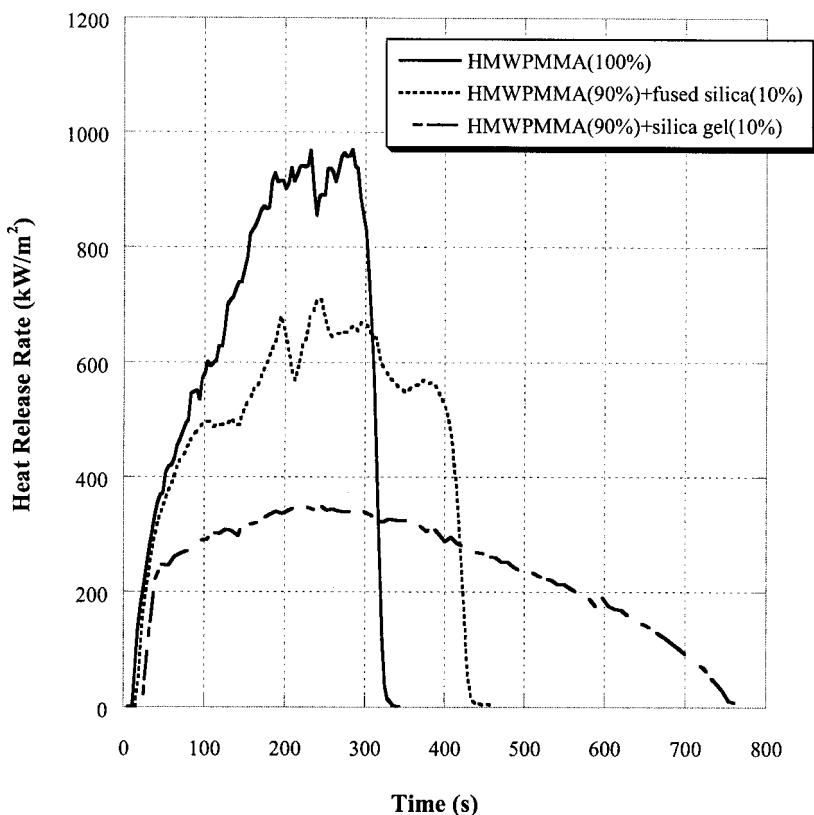
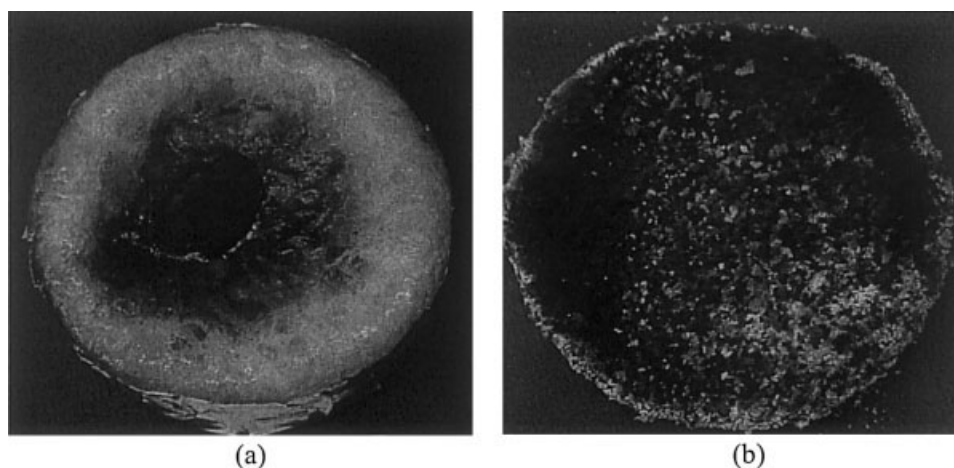


Figure 10 Effects of silica type on the heat release rate of HMWPMMA at 40 kW/m<sup>2</sup>.



**Figure 11** Pictures of collected residues when the sample lost 40% of its initial mass during the gasification experiment at  $40 \text{ kW/m}^2$  in nitrogen: (a) LMWPMMA/fused silica and (b) LMWPMMA/silica gel.

behaved like a liquid, with vigorous bubbling similar to that of the pure LMWPMMA sample. The silica gel particles used in this study had large pore volumes and surface areas and had the appearance of fluffy, light feathers. The addition of the silica gel significantly increased the melt viscosity of both LMWPMMA and HMWPMMA, in particular, for LMWPMMA. The melt viscosity of the LMWPMMA/silica gel sample was about the same as that of the HMWPMMA/fused silica sample at high temperatures. Addition of the fused silica to the HMWPMMA sample resulted in neither large bubble formation nor a fluid surface but rather the formation of a frost-like surface with white islands.

To determine the fate of the silicas in these PMMA samples during the gasification, sample residues were collected by termination of the tests when each sample lost about 40% of its initial mass. It took about 325 s of exposure for LMWPMMA/fused silica and about 420 s of exposure for LMWPMMA/silica gel. Pictures of the collected residues for both samples are shown in Figure 11. The residue of LMWPMMA/fused silica appeared to be a hard brittle material, once melted, with numerous large bubbles throughout the whole sample volume, and this indicated that the whole sample was melted by the end of the test (325 s). The residue of LMWPMMA/silica gel formed a bulging

crust layer roughly 1 cm thick (the entire residue was bulged upward). Its surface was covered by black granular coarse particles, and deeper layers below the surface contained numerous small pores, indicating some degradation occurred in the deeper layers. Small amounts of samples were collected from different locations in the residues for further analysis of their Si, C, and H contents. The results of the analyses are shown in Table I. The measured Si content of the top outer portion of the sample [white color portion as shown in Fig. 11(a)] of LMWPMMA/fused silica was slightly higher than the original Si content of the starting sample (about 4.4% mass fraction); also, there was no significant accumulation of fused silica in the bottom layer. It was of interest to us to know where the fused silica was in this residue. Many more segments were collected from the residue of another LMWPMMA/fused silica sample that had a 40% mass loss. Each of the segmented samples was pyrolyzed in a muffle furnace in air at  $900^\circ\text{C}$ . At the end of the test, white power (fused silica) was observed at the bottom of a crucible, and its weight was measured. The top black layer, similar to the one shown in Figure 11(a), contained about 30% silica, the top outer portion contained about 13% silica, the circumference of the residue (along the aluminum foil container edges) contained about 13% silica, and the rest of the residue

**TABLE I**  
Si, C, and H Contents in the Portions of the Residue Collected at Different Locations of the LMWPMMA Samples when the Sample Lost 40% of its Initial Mass in the Gasification Experiment at  $40 \text{ kW/m}^2$  in Nitrogen

Sample identification	Si (mass fraction %)	C (mass fraction %)	H (mass fraction %)
Top outer portion, with fused silica	$6.2 \pm 0.3$	$52 \pm 5$	$7.4 \pm 0.7$
Bottom center, with fused silica	$5.1 \pm 0.2$	$53 \pm 5$	$7.6 \pm 0.7$
Top granular particles, with silica gel	$42 \pm 2$	$6.2 \pm 1$	$0.8 \pm 0.1$
Layer immediately below the granular particles, with silica gel	$12.4 \pm 0.5$	$44 \pm 4$	$5.9 \pm 0.5$
Bottom layer, with silica gel	$4.3 \pm 0.2$	$53 \pm 5$	$7.3 \pm 0.7$

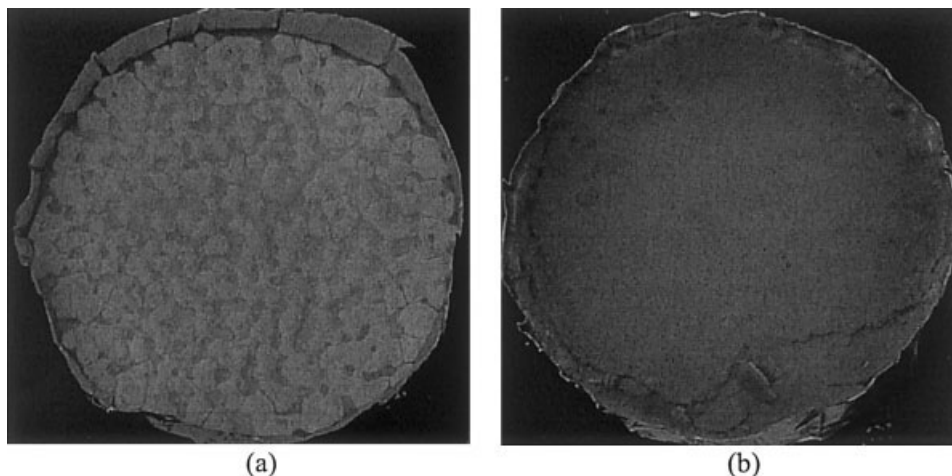


**Figure 12** Pictures of collected residues when the sample lost 40% of its initial mass during the gasification experiment at 40 kW/m<sup>2</sup> in nitrogen: (a) HMWPMMA/fused silica and (b) HMWPMMA/silica gel; the imperfections in the lower part of the residue were accidentally caused after the test.

contained about the same amount of silica as the original sample. The small accumulation of silica along the circumference could be due to the vigorous bubbling through out the molten layer, which transported silica particles radially outward and downward along the foil wall. These results indicate that for LMWPMMA/fused silica, accumulation of silica near the sample surface was not significant so the molten polymer was always available near the surface to degrade during the gasification test and the degradation products evolved without any significant obstruction. We propose that this is the reason the addition of fused silica to LMWPMMA did not reduce by any significant amount the gasification rate and heat release rate of LMWPMMA.

A significant accumulation of silica was observed in the granular particles on the top layer of the LMWPMMA/silica gel sample. Furthermore, some accumulation of silica was also observed in the layer immediately below the granular particles. Because the surface on the LMWPMMA/silica gel was covered by loose granular particles made of mainly silica, part of the virgin layer of the sample was still exposed to external radiation through the porous particles layer, and also, the barrier performance of the surface to contain the degradation products of PMMA was not effective. However, the accumulating granular parti-

cles layer acted as a mainly inert layer (PMMA was not readily available near the surface) and also as a heat insulation layer. We propose that this is the reason the addition of silica gel to LMWPMMA reduced by a relatively significant amount the gasification rate and heat release rate of LMWPMMA.

For HMWPMMA, the pictures of the samples collected after about 40% of mass loss from the initial mass in the gasification experiment are shown in Figure 12. The HMWPMMA/fused silica sample showed white, mainly connected islands covering the surface and valleys between the islands. The islands looked like singed particles. The sample below the top surface did not show pores or signs of melting, and it appeared to be the original sample material. The Si, C, and H analysis of the islands indicated that the islands were mainly silica, and the valley was a composition similar to the original sample, as shown in Table II. It is of interest how this surface pattern was formed during the gasification experiment. There are two likely mechanisms; one would be due the diffusion of the particles in the polymer melt layer (a similar pattern was observed in a gel<sup>11</sup>); the second would be the bursting of bubbles at the surface, which pushed the particles away from bubbles, and the particles accumulated locally and formed "singed" islands. The formation of the silica islands significantly reduced the

**TABLE II**  
Si, C, and H Contents in the Portions of the Residue Collected at Different Locations of the HMWPMMA Samples when the Sample Lost 40% of its Initial Mass in the Gasification Experiment at 40 kW/m<sup>2</sup> in Nitrogen

Sample identification	Si (mass fraction %)	C (mass fraction %)	H (mass fraction %)
Top white islands on surface, with fused silica	45 ± 2	4 ± 1	0.5 ± 0.1
Valleys between the islands, with fused silica	7.0 ± 0.3	52 ± 5	7.4 ± 0.3
Top layer, with silica gel	43 ± 2	5 ± 1	0.7 ± 0.1
Layer 3 mm below, with silica gel	6.3 ± 0.3	52 ± 5	7.2 ± 0.7

availability of HMWPMMA for degradation near the surface, but the islands did not cover the entire surface. The valleys were exposed to the external radiation and continued to degrade so that the addition of fused silica to HMWPMMA reduced the gasification rate and heat release rate but not as much as was the case for the HMWPMMA/silica gel (the entire surface was covered by a silica net as described later).

The picture of the collected residue of HMWPMMA/silica gel after about 40% mass loss showed a smooth surface without any formation of bubbles or any significant regression, as shown in Figure 12(b). The top layer (about 3 mm thick) was of a soft, fine texture, which covered the entire surface. The sample below the layer did not show any pores or signs of melting, and it appeared to be the same as the unexposed original sample material. The top layer consisted mainly of silica, as shown in Table II. Because no significant sample surface recession was observed over the entire gasification experiment, the silica gel particles probably formed a continuous silica gel net. A similar top layer was also formed for the PP/silica gel sample during gasification experiments, and progressive accumulation of silica near the surface was observed with the progress of those experiments.<sup>5</sup>

The accumulation of silica near the sample surface during gasification or burning has four important effects on the mass loss rate in nitrogen or on the heat release rate (burning rate): first is the depletion of PMMA (or any volatile organic material) concentration near the sample surface, second is the formation of a thermal insulation layer, third is the formation of a barrier for the evolved degradation products to the gas phase, and fourth is the change in surface reflection characteristics with respect to the incident radiation. Theoretical models of polymer gasification with an inert additive in the sample predict a significant reduction in the mass loss rate by the depletion of the polymer concentration near the surface with the accumulation of inert silica.<sup>5,12</sup> The second effect has been clearly demonstrated by the measurement of heat transfer rate through silica ash layers of various thicknesses. A reduction of roughly 65% of incident radiant flux was reported with a 1.5-mm layer of silica ash.<sup>13</sup> The third effect appears as the formation of the solid-like sample surface without melting and vigorous boiling. The transport of the degradation products from the interior of the sample to the sample is very rapid during a boiling process. With the formation of the layer, the transport process appears to be capillary through the particle-filled solid-like layer. The capillary transport is slower than that through boiling. The fourth effect is the increase in surface reflectance with respect to the incident radiation with an increase in scattering from the accumulated silica compared to more absorbing PMMA.

There might be some change in PMMA degradation reactions due to the entrapment/entanglement of polymer chains with silica gel particles having a large pore volume and surface area, hydrogen bonding with silanol, or dipole-dipole coupling between the carbonyl of PMMA and Si-O bonds.<sup>14</sup> If crosslinks are followed by the formation of a carbonaceous network (char), a combined layer consisting of accumulated silica gel particles interspersed with the char network would be formed. Such a layer would have more physical integrity and would be a better protective layer.<sup>3</sup> Such a layer might not be formed in the thermogravimetric analysis (TGA) experiment when a sample weight of less than 10 mg (little accumulation of silica within an extremely thin sample layer) is used, and no significant change in thermal stability of PMMA by the addition of the silica gel was observed, except for the formation of the first mass loss peak, as shown in Figure 2. Although the temperature range was higher than that used in this study (up to 500°C), it was reported that high yields of mesoporous carbon were generated from furfuryl alcohol with high-surface-area silica particles at a heating rate of 2.5°C/m to 800°C in nitrogen flow and held there for 3 h.<sup>15</sup> It appears that something analogous could be the case for the HMWPMMA/silica gel samples, which generated some carbonaceous residue during the gasification. TGA analysis, in a nitrogen atmosphere, of the residues collected after gasification tests showed that the mass loss rate of the residue of the HMWPPA/silica gel was very small, even at 1000°C, without any distinct mass loss rate peak. However, a high mass loss rate from the residue of the LMWPMMA/silica gel was observed from 500°C on upward, and a broad peak was observed around 620°C.

The gasification rate and heat release rate of all silica/PMMA samples showed no significant difference from those of pure PMMA samples at the early stages of the test, as shown in Figures 6 and 8–10, even with the best performer (i.e., the HMWPMMA/silica gel sample). A silica mass fraction of 10% in PMMA appeared to be insufficient to reduce the early mass loss rate or heat release rate. With the progress of the test, polymer resins degraded and depleted and the accumulation of light silica particles occurred. Thus, the silica concentration near the sample surface increased with the progress of the test. Our previous study showed that an increase in silica gel concentration in the initial sample enhanced early reduction of mass loss rate in a PP/silica gel system.<sup>5</sup> At a low concentration of silica gel in PP, many solid-like islands were formed during the gasification test instead of a solid-like surface covering over the entire sample surface. Melting and bubbling were observed in the valleys among the islands.

## CONCLUSIONS

For PMMA, the addition of silica particles with high surface area and large pore volume increased the melt viscosity and significantly reduced the mass loss and heat release rates, even for LMWPMMA. The HMWPMMA with the silica gel had the lowest mass loss rate and heat release rate in this study. However, the addition of fused silica particles with low surface area to LMWPMMA did not reduce the mass loss rate and heat release rate of PMMA. The HMWPMMA with fused silica and the LMWPMMA with silica gel had a lower mass loss rate and heat release rate than the PMMA without any silica additives. The results of the species composition analysis of the collected residue samples at about 40% mass loss in the gasification experiments and observation of degrading samples showed that the accumulation of silica near the surface and its extent of covering the surface (entire surface vs. partial covering) had significant effects on the reduction of mass loss rate and heat release rate of PMMA. The LMWPMMA/fused silica sample did not form significant accumulation of silica near the surface due to radial outward transport of fused silica particles by convection caused by vigorous bubbling (due to the low viscosity of the molten layer). The LMWPMMA/silica gel sample and the HMWPMMA/fused silica formed silica-filled particles or islands on the surface, but they did not cover over the entire surface. The HMWPMMA/silica gel formed a silica gel net layer covering the entire surface. The two critical quantities, amount of accumulation of silica particles, and their extent of covering the surface were determined by not only the silica characteristics but also by the melt viscosity of PMMA. This confirms that the relation between the melt viscosity of a polymer and

surface area/pore volume of silica particles has significant effects on flammability properties.

The authors thank Alexander Morgan, Siaka Yusuf, and Bryan Haskins of Dow Chemical Co. for their help with the chemical composition analysis of the collected residues.

## References

1. Lyons, J. W. *The Chemistry and Uses of Fire Retardants*; Wiley-Interscience: New York, 1970.
2. Gilman, J. W.; Kashiwagi, T.; Lichtenhan, J. D. *SAMPE J* 1997, 33, 40.
3. Kashiwagi, T.; Gilman, J. W. In *Fire Retardancy of Polymeric Materials*; Grand, A. F. Wilkie, C. A., Eds.; Marcel Dekker: New York, 2000; Chapter 10.
4. Gilman, J. W.; Jackson, C. L.; Morgan, A. B.; Harris, R. H., Jr.; Manias, E.; Giannelis, E. P.; Wuthenow, M.; Hilton, D.; Phillips, S. H. *Chem Mater* 2000, 12, 1866.
5. Kashiwagi, T.; Gilman, J. W.; Butler, K. M.; Harris, R. H.; Shields, J. R. *Fire Mater* 2000, 24, 277.
6. Kashiwagi, T.; Hirata, T.; Brown, J. E. *Macromolecules* 1985, 18, 131.
7. Gilman, J. W.; Kashiwagi, T.; Nyden, M.; Harris, R. H. Jr. *New Flame Retardants Consortium: Final Report—Flame Retardant Mechanism of Silica*; NISTIR 6357; NIST: Gaithersburg, MD, 1999.
8. Austin, P. J.; Buch, R. R.; Kashiwagi, T. *Fire Mater* 1998, 22, 221.
9. Kashiwagi, T.; Inaba, A.; Brown, J. E.; Hatada, K.; Kitayama, T.; Masuda, E. *Macromolecules* 1986, 19, 2160.
10. Madorsky, S. L. *Thermal Degradation of Organic Polymers*; Interscience: New York, 1964; Chapter 8.
11. Tanaka, T.; Fillmore, D. J.; Sun, S.-T.; Nishio, I.; Swislow, G.; Shah, A. *Phys Rev Lett* 1980, 45, 1636.
12. Staggs, J. E. *Fire Safety J* 1999, 32, 221.
13. Hshieh, F.-Y. *Fire Mater* 1998, 22, 69.
14. Landry, C. J. T.; Coltrain, B. K.; Wesson, J. A.; Zumbulyadis, N.; Lippert, J. L. *Polymer* 1992, 33, 1496.
15. Kawashima, D.; Aihara, T.; Kobayashi, Y.; Kyotani, T.; Tomita, A. *Chem Mater* 2000, 12, 3397.